In-Flight Investigation of Large Airplane Flying Qualities for Approach and Landing

Norman C. Weingarten* and Charles R. Chalk†
Arvin/Calspan Advanced Technology Center, Buffalo, New York

A study of the handling qualities of large airplanes in the approach and landing flight phase was performed utilizing the Total In-Flight Simulator. A 1 million lb statically unstable airplane model was used as a baseline about which variations were made. The primary variables were relative pilot position with respect to center of rotation, command path time delays and phase shifts, augmentation schemes, and levels of augmentation. The results indicate that the approach and landing task with very large airplanes is a fairly low bandwidth task. Low equivalent short-period frequencies and relatively long time delays can be tolerated. As the pilot position is moved aft toward and then behind the center of rotation, pilot ratings are degraded.

Introduction

THE objective of this in-flight research program was to obtain data applicable to flight phase category C operation of class III airplanes, that is, approach and landing task for very large (1 million lb), low load factor airplanes.

The primary variables in the large airplane longitudinal experiments were:

1) Pilot location with respect to pitch center of rotation presented as three different aircraft design configuration—long aft tail, canard, and short aft tail.

2) Augmentation schemes—α feedback or q feedback with proportional plus integral in the direct path.

3) Level of augmentation—from statically unstable to level 1 stability.

4) Time delay—produced by model-following lags and inserted prefilters and pure time delays in the command path.

Three different aircraft designs were generated to evaluate pilot position vs instantaneous center-of-pitch rotation. The aerodynamics and control systems of all of these configurations were essentially the same, except for the values of lift and moment due to elevator deflection which were used to shift the center of rotation. The three basic configurations were (see Fig. 1): long aft tail: a generic conventionally designed aircraft; canard: pitching moment controller forward, shifting the center of rotation aft, similar to a slender arrow-wing supersonic cruise design with a canard; and short aft tail: a generic delta wing design with elevons for pitch and roll control, shifting the center of rotation forward of the pilot, similar to the Space Shuttle Orbiter design. The location of the cockpit relative to the center of gravity was also varied for each of the configurations.

Combined with the three basic configurations were two different types of pitch augmentation systems; an angle of attack feedback system (Fig. 2) and a pitch rate feedback system (Fig. 3). Control system gains were varied to augment the statically unstable basic airframe toward level 1 handling qualities.

Included in the command paths were different levels of extra transport delays (representative of digital control systems) and first-order prefilters (representative of structure filters). The experiment and extensive analysis of the results are reported in Ref. 1.

Received Aug. 4, 1982; presented as Paper 82-1296 at the AIAA 9th Atmospheric Flight Mechanics Conference, San Diego, Calif., Aug. 9-11, 1982; revision received March 14, 1983.

*Principal Engineer. Member AIAA.
†Staff Engineer. Member AIAA.

Experiment Design

Configuration Description

This flight research program consisted of six sets of longitudinal configurations, which are outlined and illustrated by the following discussion and table. Configuration sets 1, 2, and 3 were intended to explore the interactions of basic configuration factors together with an angle-of-attack loop. The α augmentation system is shown in Fig. 2. The α signal used was derived in a way which eliminated direct turbulence effects on the feedback signal. The α feedback gain was varied, along with the effective time delays in the pilot's command path to the elevator. The q augmentation parameters (K_q and T_q) on Fig. 3 were selected to give sets 4, 5, and 6 with augmented dynamics analogous in an "equivalent system" sense to the short-period dynamics of the α-augmented configurations of sets 1, 2, and 3. The K_q gain was inversely proportional to dynamic pressure, $\bar{q}$, to keep the dynamics constant when speed changed.

The configuration sets are defined in Table 1.

$T_q = 1.0$ for sets 4, 5, and 6, except for the extra-high K_q configurations for which $T_q = 0.50$.

$T_{l_{\text{pitch}}}$ is the nominal effective time delay ($A = 0.06$, $B = 0.13$, $C = 0.2$ s). X_{mp} and X_{PCR} refer to the pilot position with respect to the center of gravity and center of rotation, respectively.

In addition to the above configurations, which were flown at their respective nominal pilot positions, a few extra evaluations were flown with the pilot position shifted.

Long aft tail, high q, $X_{mp} = 50$ ft, $X_{PCR} = 32.5$ ft

Canard aft tail, high q, $X_{mp} = 50$ ft, $X_{PCR} = 80$ ft

Short aft tail, high q, $X_{mp} = 70$ ft, $X_{PCR} = 10$ ft

Short aft tail, high q, $X_{mp} = 110$ ft, $X_{PCR} = 50$ ft

These were all run with $T_{l_{\text{pitch}}} = 0.06$.

Equipment

The Total In-Flight Simulator (TIFS) was used as the test vehicle in this experiment. TIFS is a highly modified C-131 (Convair 580) configured as a six degree-of-freedom

simulator (Fig. 4). It has a separate evaluation cockpit forward and below the normal C-131 cockpit. When flown from the evaluation cockpit in the simulation or fly-by-wire mode, the pilot control commands are fed as inputs to the model computer which calculates the aircraft response to be reproduced. These responses, along with TIFS motion sensor signals, are used to generate feed-forward and response error signals which drive the six controllers on the TIFS. The result is a high-fidelity reproduction of the motion and visual cues at the pilot position of the model aircraft. A detailed description of the TIFS can be found in Ref. 2.

Simulation Geometry

The TIFS motion system was configured to reproduce the model's motion at the evaluation pilot's eyepoint as if the TIFS were positioned as shown in Fig. 5. In this sketch, the model is shown in its approximate attitude at touchdown. Despite qualms about the possible effect on pilot rating of not actually touching down, it was decided to preserve the proper geometric relationship between the pilot and main gear at touchdown. Altitude was measured by a radar altimeter mounted on the underside of the TIFS fuselage.

Evaluation Cockpit Configuration

The evaluation cockpit was configured with the evaluation pilot in the left seat with wheel-column and rudder pedals. The four throttle levers were active and commanded the total thrust of all four engines on the model without any yawing moment effects; that is, each throttle lever controlled one fourth of the input to the total thrust computation. This provided a large-airplane feel without added computational complexity.

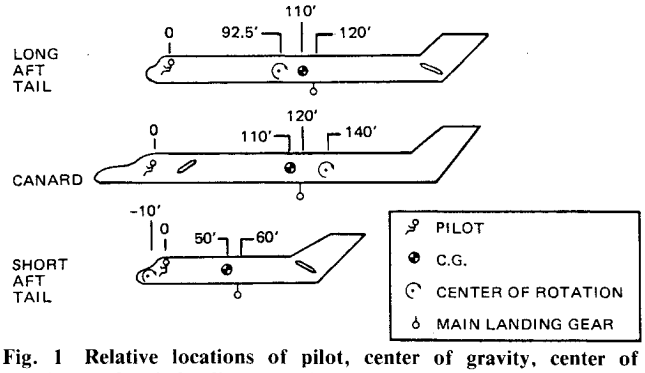

Fig. 1 Relative locations of pilot, center of gravity, center of rotation, and main landing gear of various base configurations.

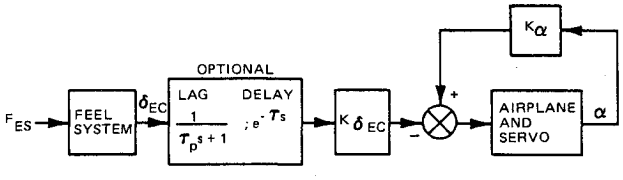

Fig. 2 Angle-of-attack augmentation.

Evaluation Procedure and Task Description

The approach and landing evaluation task, following some brief airwork, consisted of the following: Precision tracking of the instrument landing system (ILS) beam, preceded by a "capture" segment beginning beyond the outer marker and at an angle between 30-45 deg to the beam. The evaluation pilot was "under a hood" during the simulated instrument flight rules (IFR) approaches until the final portion starting from the middle marker at an altitude of approximately 300 ft down to the completion of the task. This latter portion of the approach including flare and a simulated touchdown at proper model eye height of 43 ft was to be completed visually. Precise simulated touchdowns were to be attempted. Acceptable landings were defined to be within a 1000-ft zone centered 1000 ft from the threshold of the runway and with a low sink rate (5 ft/s). Touchdown was signaled by a tone over the intercom and a signal light.

The task was made more difficult with the addition of localizer offsets and artificial or natural atmospheric disturbances of crosswinds and turbulence. The localizer offset was a constant 1.5 deg or 1.2 dot angular offset that translated to a 400-ft lateral error at the breakout altitude of 300 ft. This forced the pilot to make lateral-directional corrections, so all of his attention was not kept on the longitudinal task. The crosswind was added or canceled out with the TIFS sideslip mismatch capability. This capability is limited to a β of 0.1 rad, equivalent to a 15 knot change in the apparent crosswind at an airspeed of 150 knots. Turbulence was also added to disturb the model's response. It was desired to have a light-to-moderate level of turbulence during each evaluation. When the natural level of turbulence was at this level, it was measured and introduced into the model's aerodynamic equations through α_g and β_g components, but not into the α or β sensors of the model. When the natural

Table 1 Configuration matrix

	Long aft tail	Canard	Short aft tail
X_{mp},	110	110	50
X_{PCR}, ft	92.5	140	−10
Time delay			
$T_{l_{pitch}}$	A B C	A B C	A B C
K_{re}	Set 1	Set 2	Set 3
0	X X	X X	
Low	X X X	X X X	
Medium	X X X	X X X	X X
High	X X X	X X X	X X
Extra high	X	X	
K_q	Set 4	Set 5	Set 6
Low	X X		
Medium	X X X		X
High	X X X	X	X
Extra high			X

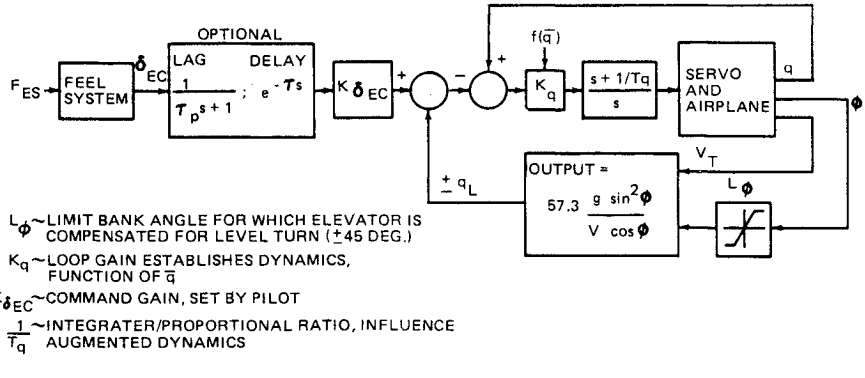

Fig. 3 Pitch rate augmentation system.

level of turbulence was less than this, artificially generated turbulence was introduced into the model. The turbulence signals recorded on an FM recorder are filtered Gaussian white noise. The filtered noise approximates a Dryden model of turbulence at one specific altitude and speed. The filter characteristics, described in Ref. 1, were chosen to duplicate a Dryden power spectrum of turbulence at 330 ft and 150 kias.

Pilot comments and Cooper-Harper ratings[10] were given after each evaluation.

Results of the Experiment

The results of the experiment are extensively analyzed and reported in Ref. 1. This paper will briefly discuss airspeed control problems and the effects of pilot location relative to the center of rotation. The effects of augmentation and time delay are treated through closed-loop analysis.

Airspeed Control

The pilots noted problems with airspeed control on about two thirds of the evaluations. These occurred less often with q augmentation than with α augmentation and the problems were less severe for the higher augmentation gains than for the lowest gain configurations and the unaugmented airplane. There may have been a one or two point degradation in pilot rating due to the speed control problem. A number of factors can be identified which contributed to the airspeed control problems. The configurations were slightly on the backside, requiring active control of airspeed and thrust management in turns. The lag in thrust buildup following throttle inputs was long (a 3-s time constant) and the throttle position for trim was difficult to find. Together with turbulence, these factors caused airspeed to wander and made the response to throttle difficult to predict.

Pilot Location Effects

Figure 6 shows how pilot ratings were affected by the variation of pilot position with respect to pitch center of rotation. The pilot position was varied from 10 ft aft of the center of rotation in the short aft tail configuration to 140 ft forward in the canard. The data presented in Fig. 6 are only the high level of augmentation cases with the low time delay level, $T_I = 0.06$. Though there is some variability in pilot ratings at each value of X_{PCR} due to augmentation system and airspeed control problems, there is a definite trend toward better ratings as the pilot is positioned further forward of the center of rotation. The differences in pilot ratings between the long aft and short aft tail configuration are generally 3 to 5.

This large variation in pilot ratings for configurations that were essentially the same except for pilot position is partly the effect of visual perception of rate of climb and altitude at the pilot position when near the ground and partly the effect of normal acceleration felt by the pilot. These cues are the normal acceleration at the pilot station and essentially the integrations of it. Normal acceleration at the pilot station is defined by:

$$n_{z_p} = n_{z_{c.g.}} + \frac{X_{mp} q}{g}$$

Figure 7 presents the normal acceleration and altitude step responses for the three configuration designs, each for the high-a augmentation level. It can be seen that the canard configuration has a 50% larger initial n_{z_p} kick than the long aft tail configuration. The short aft tail design produces nonminimum-phase shape with the response initially going slightly negative before going positive and matching the other

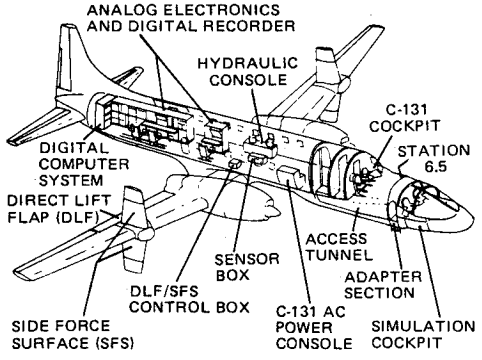

Fig. 4 Total in-flight simulator (TIFS).

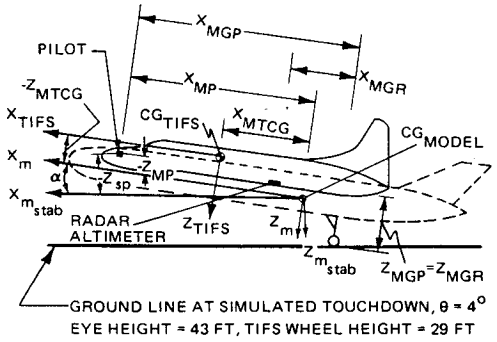

Fig. 5 Geometry of TIFS superimposed on model.

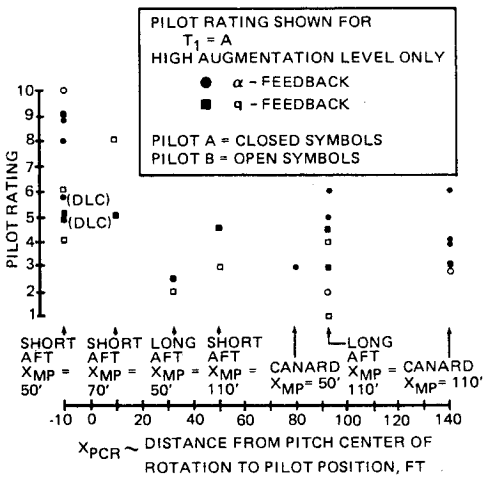

Fig. 6 Pilot rating vs pilot position—center of rotation (X_{PCR}).

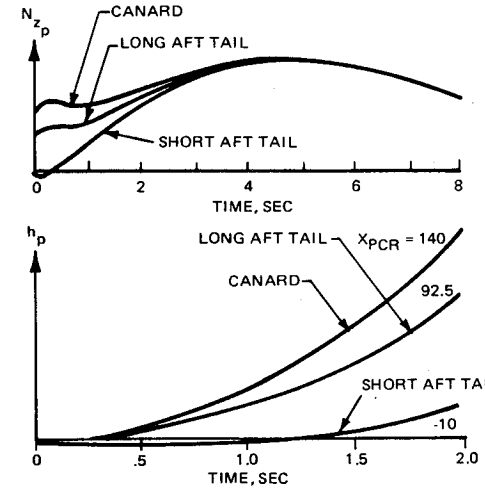

Fig. 7 Normal acceleration and altitude at pilot station responses to step input, high α augmentation, $T_I = A$.

responses near 3 s into the time history. It is near 1½ s into the response before the pilot can actually see his altitude change. The pilot comments clearly indicate that the pilots perceived this. With the canard configuration, the pilots found they could fly the airplane more "naturally," the response felt more crisp, and fine corrections in sink rate near touchdown were easily made. These comparisons are with respect to the long aft tail configuration. The better perceived control over rate of sink, especially in the flare, overcame some of the problems related to the low short-period frequency, observed with the long aft tail design. The short aft tail design was described as "very sluggish and delayed," even with the high augmentation levels and no extra lags or delays added. The ILS and visual flight rules (VFR) tracking away from the ground was described as "all right," but as soon as the pilot acquired outside cues for references in flare and touchdown the control deteriorated. Many times, pilot induced oscillations (PIOs) resulted. Comments indicated precise control of sink rate near touchdown was very poor or impossible. All of the pilot's attention was devoted to the altitude and rate of sink task with the touchdown-point and lateral-directional task ignored many times.

Pitch Attitude Pilot-Airplane Closed-Loop Analysis

The effects of time delay, augmentation type, and level of augmentation were treated through closed-loop analysis. The pitch attitude control loop structure used in the analysis is illustrated by the block diagram in Fig. 8.

The analysis is derived from the work by Neal and Smith reported in Ref. 3. The basic approach is to model the pilot-airplane pitch attitude control loop as a unity feedback system with a pilot model of an assumed form in the forward loop.

The pilot model used is

$$Y_{P_\theta} = K_{P_\theta} e^{-0.25\,s} \frac{5s+1}{s} (\tau_L s + 1)$$

The gain, K_{P_θ}, is in units of lb/rad.

The $e^{-0.25\,s}$ term accounts for time delay in the pilot's neuromuscular system. The value of 0.25 s is based on delays observed in records for the discrete tracking task performed in Refs. 3 and 4. These records exhibit delays ranging from 0.20 to 0.40 s. The value of 0.25, selected on the basis of cut and try data correlation, is interrelated with the bandwidth frequency that is specified for a given flight phase or task.

The $5s+1/s$ term provides low-frequency integration capability. A form of the pilot model *without* this term can be used when *constant speed* or *two-degree-of-freedom* equations are used to represent the airplane. In that case, the airplane transfer function should have a free s in the denominator and low-frequency integration by the pilot will not be necessary. When three-degree-of-freedom equations are used, as is the case in the present analysis, or when the flight control system uses high gain attitude stabilization, it is hypothesized that the pilot model performs low-frequency integration to avoid droop at frequencies less than ω_{BW}. The 5-s lead term permits using integration to avoid the droop limit at low frequency while not significantly affecting the short-term dynamics of primary interest.

The $(\tau_L s+1)$ term accounts for the lead that the pilot provides to achieve desired closed-loop performance and is a measure of his workload. None of the configurations in this experiment required lag equilization.

It is hypothesized that a given flight phase or task performed in a typical environment will require certain minimum dynamic characteristics of the closed-loop pilot-airplane system. The parameters used to define the closed-loop dynamic performance are bandwidth, droop at frequencies below the bandwidth, and resonance magnitude. These closed-loop system parameters are defined by the curved lines on Fig. 9.

The maximum droop permitted for $\omega<\omega_{BW}$ is -3.0 dB. This value, defined somewhat arbitrarily, can be justified from examination of discrete tracking task records in Refs. 3 and 4 and by interpretation of pilot comments in these references. The closed-loop system resonance limits for levels 1 and 2 have been determined from empirical data correlation in Refs. 3-6. The bandwidth frequency, defined as the frequency which results in a closed-loop phase of -90 deg, is dependent upon the task and is interrelated with the pilot time delay assumed.

Pilot Compensation (Neal-Smith) Analysis

The pilot lead compensation $(\tau_l s+1)$ was calculated which would make the open-loop compensated-pilot plus aircraft transfer function (θ/θ_ϵ), drawn on a Nichols diagram, pass through the acceptable closed-loop criteria region (see Fig. 9); that is, find the appropriate gain and lead to keep closed-loop droop less than -3 dB for $\omega<\omega_{BW_\theta}$ and closed-loop resonance less than $+3$ dB. The bandwidth chosen for this set of data was 1.5 rad/s. This value of bandwidth resulted from correlation of the $PR=3.5$ data with pilot lead compensation of approximately 45 deg or less. This value of bandwidth appears appropriate for the task of landing a very large transport in a manner which does not require high agility of the closed-loop pilot-airplane system.

To obtain the pilot compensation, lead was added to force the 1.5 rad/s point through the -90 deg closed-loop phase line with the θ/θ_ϵ plot just skimming the $+3$ dB closed-loop resonance boundary. The resulting closed-loop droop was much less than -3 dB (near 0 dB) for most configurations. Lower resonance could have been obtained with the droop still not dropping below -3 dB by using more lead compensation. The solutions chosen, therefore, usually represented minimum pilot lead required to meet the per-

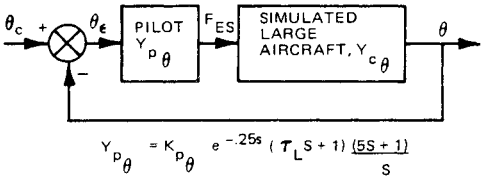

Fig. 8 Pitch attitude control-loop structure.

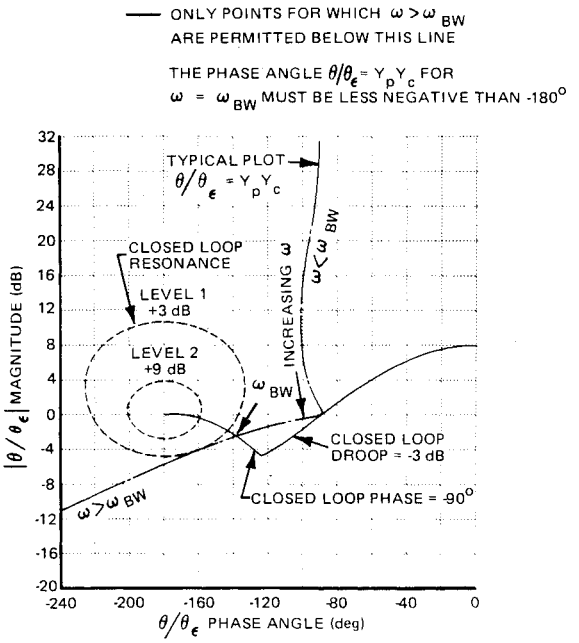

Fig. 9 Design criteria for pitch dynamics with the pilot in the loop.

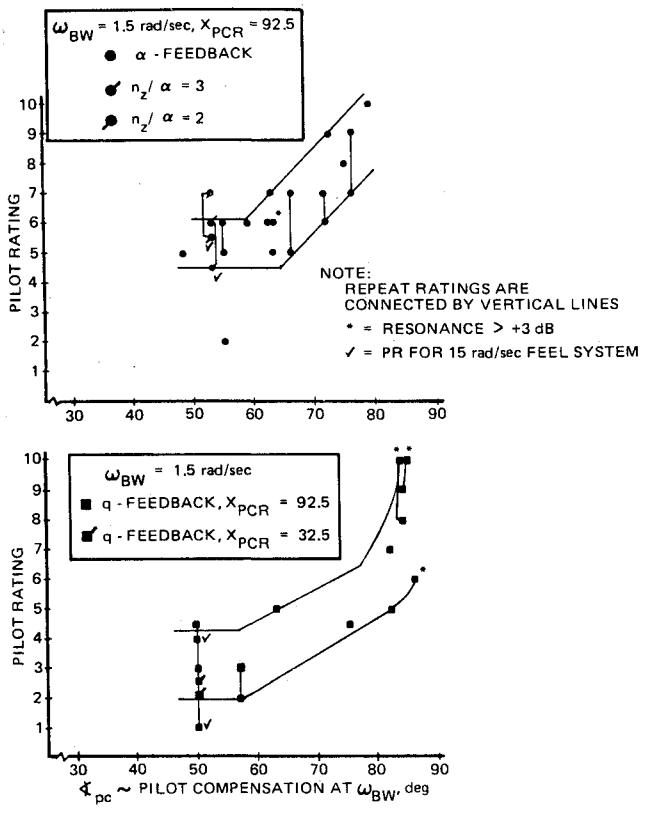

Fig. 10 Long aft tail pilot rating vs pilot lead compensation.

formance standard. For a few cases, the performance criterion of less than 3 dB resonance could not be achieved with the maximum lead permitted by the pilot model.

The aircraft plus compensated-pilot, open-loop θ/θ_c transfer functions for each configuration evaluated are presented in Ref. 1. Plots of pilot ratings vs the pilot compensation, ΔPC, are presented in Figs. 10-12 (see Ref. 1 for details).

There is a definite trend toward worse pilot ratings as more pilot compensation is required. From the long aft tail and canard configurations data, it appears that the phase compensation must be less than 55 deg for level 1 ratings and less than 75 deg for level 2 ratings. The points with large pilot compensation correspond to the configurations with low augmentation levels and extra time delays and lags added. The correlation of pilot rating and pilot compensation generally agrees with data from Refs. 3 and 5. This means that the amount of phase compensation at the bandwidth frequency required to meet the closed-loop performance criteria is a good measure of pilot acceptance of the configuration. The same values appear to be valid for fighter tasks, as well as transport approach tasks, as long as the appropriate bandwidth is chosen.

The short aft tail configurations do not appear to correlate well with these criteria. Pilot ratings up to 10 were assigned for configurations which required only 55 deg of phase compensation. The extra-high q-augmented configuration required only 17 deg of compensation, but still received a pilot rating of 4. This points out the fact that the pilot uses more than just pitch attitude in his control scheme. Normal acceleration, altitude rate, and altitude responses at the pilot position must also be important. Again for both the long aft and short aft tail configurations, the q-augmented configurations consistently received better ratings than the α-augmented ones even though the required pilot compensation was nearly the same. The q-augmented configurations exhibited reduced response to turbulence (see Fig. 13), did not require control force in turns, and the attitude hold feature

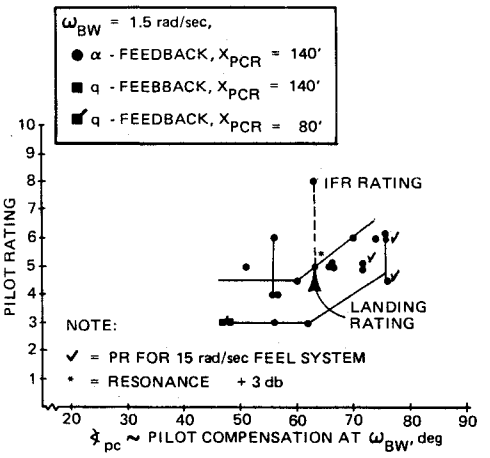

Fig. 11 Canard pilot ratings vs pilot lead compensation.

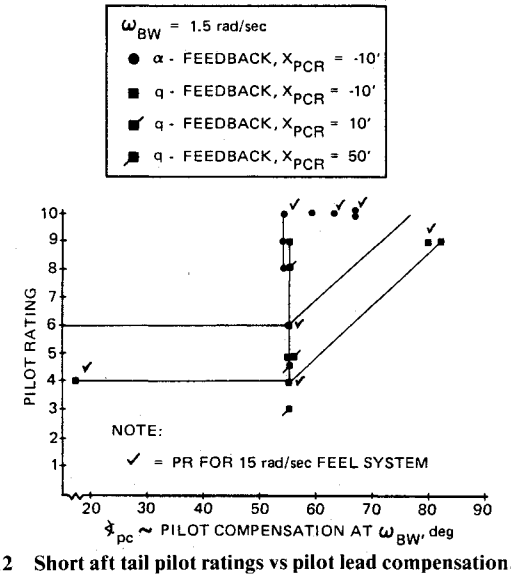

Fig. 12 Short aft tail pilot ratings vs pilot lead compensation.

rejected the pitch disturbances due to ground effect, whereas the α-augmented configurations did not.

The operation of the aircraft on the backside of the power required curve in conjunction with the slow thrust response also appears to put a limit on the best pilot ratings of approximately 3. Only rarely were pilot ratings of 2 or 1 received. The pilot downgraded otherwise good configurations due to the speed control problems.

Effect of Bandwidth on Allowable Time Delay

From previous experiments,[3,4,7] dealing with higher-order systems and their effective time delays, there appears to be a general increase in the level of time delay acceptable as the task presented the pilot becomes less difficult. Figure 14 from Ref. 6 compiles much of these data and, in particular, shows the effect of time delay on pilot ratings for three degrees of task difficulty. When the present experimental data for the long aft tail and canard high α and q-augmented configurations are pointed out on Fig. 14, they agree with the trend shown; that is, large time delays become acceptable at low bandwidth and the degradation in pilot rating resulting from the large variation of time delay used in the present experiment is less than that for higher bandwidth tasks.

A functional relationship was determined between the average tolerable effective time delay and bandwidth for the task, for pilot ratings of 9.5, 6.5, and 3.5. In the relationships derived, the allowable effective time delay, t_l, was inversely proportional to the bandwidth of the task for the various

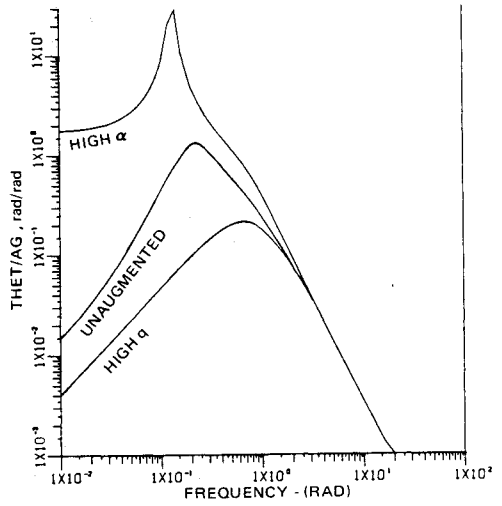

Fig. 13 Long aft tail, turbulence response, θ/α_g.

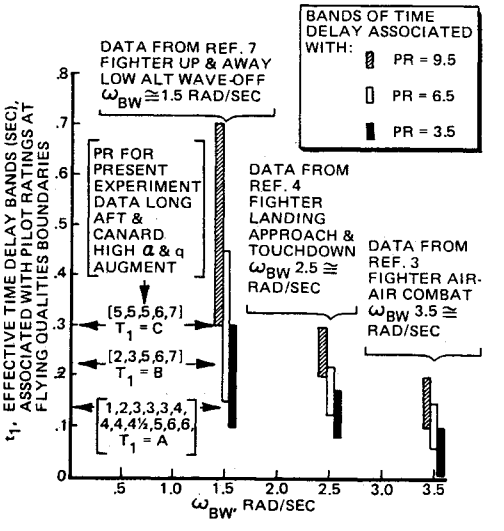

Fig. 14 Time delay bands associated with flying qualities boundaries vs bandwidth.

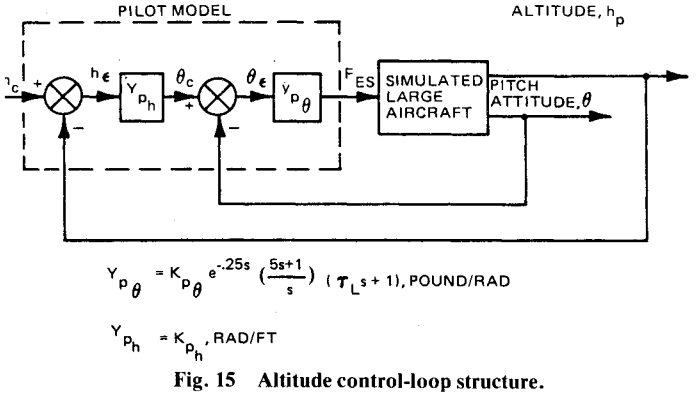

Fig. 15 Altitude control-loop structure.

flying qualities levels

At $PR = 9.5$,

$$t_l = \frac{0.65}{\omega_{BW}}$$

At $PR = 6.5$,

$$t_l = \frac{0.4}{\omega_{BW}}$$

At $PR = 3.5$,

$$t_l = \frac{0.3}{\omega_{BW}}$$

For the data from the present experiment, the average pilot ratings increased from approximately 3.5 to 6 as the effective time delay increased from 0.14 to 0.3, which tends to support the relationships shown at $\omega_{BW} = 1.5$ rad/s.

Multiloop Analysis

In order to better understand the evaluations of configurations with varying pilot position vs instantaneous pitch center of rotation with all other characteristics constant, a multiloop analysis was performed. An outer altitude control loop was added to the inner pitch attitude control loop as shown in Fig. 15. The inner-loop pilot gain (K_{P_θ}) and lead (τ_L) were fixed at the values obtained in the pitch attitude closed-loop analysis with a bandwidth of 1.5 rad/s. The pilot model for the outer loop was a pure gain, K_{P_h}, regulating the perceived altitude error, h_ϵ, at the pilot's position. The lead term in the inner loop ($\tau_L s + 1$) also provides lead in the altitude loop.

The analysis is based on the transfer functions in Ref. 1, which are evaluated at the nominal trim speed. Complete transfer functions were used without simplification or approximation. The time delays were treated in $e^{-\tau s}$ form. The computer program developed in Ref. 8 was used to calculate root loci, and Nichols diagrams were used to determine closed-loop bandwidth. It is noted that all of the configurations have a low-frequency factor in the numerator of the altitude-elevator transfer function that is in the right half plane as a result of being on the "backside." The analysis performed considered multiple feedback to a single controller, the elevator. This loop closure results in a low-frequency pole of the closed-loop system being driven toward the low-frequency zero of the altitude-elevator transfer function, and in all of these configurations this root was unstable.

In order to stabilize this closed-loop pole, it would be necessary to close a low gain feedback loop of airspeed to the throttle. This loop closure was not included in the analysis, and the results described in the following paragraphs must be viewed with that fact in mind.

Although the closed-loop system transfer function was 11th order over 15th order and included time delay, the results of the analysis will be discussed in terms of the dominant set of complex roots of the closed-loop altitude-to-stick-force dynamic system.

The root locus analysis for the short aft tail configurations shows that when the pilot is behind the center of rotation, the altitude transfer function has a zero in the right half plane and the altitude mode goes unstable. When the pilot station is moved forward, this zero moves to the left half plane and the closed-loop system exhibits higher bandwidth and stability. The potential closed-loop bandwidth is thus higher at the more forward pilot locations. Low bandwidths of the altitude loop correlate highly with the occurrence of PIOs near touchdown for the short aft tail. The zeros of the altitude transfer function for the long aft tail and canard configurations are in the left half plane and the altitude mode does not go unstable with increased altitude-loop gain.

The Nichols analysis for these configurations shows that the highest achievable bandwidth for the altitude control loop increased from 0.43 to 2.30 rad/s as the pilot position was moved from 10 ft aft to 140 ft forward of the center of rotation. The largest increase occurred going from the long aft tail to the canard configuration. It is noted that the pilot lead used for the inner loop (τ_L) had a significant effect on the bandwidth of the altitude loop and pilot lead; when added in the outer altitude loop, it allowed further increase in bandwidth.

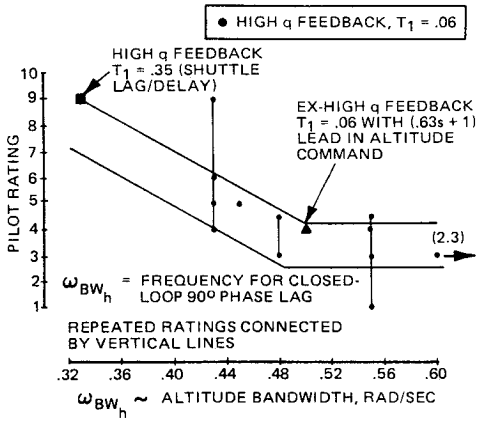

Fig. 16 Pilot ratings vs altitude bandwidth.

Pilot ratings are correlated with the calculated altitude loop bandwidth in Fig. 16; the trend toward better ratings with high bandwidth can be seen. Though not enough samples were taken to absolutely define flying qualities boundaries, it appears that a bandwidth of greater than 0.5 rad/s may be necessary for level 1 ratings. This correlates well with data in Ref. 9, where the same altitude control-loop pilot model was used to analyze data from a medium transport landing approach experiment.

Conclusions

1) The pilot rating and comment data presented for a 1 million lb airplane exhibit significant effects of the following experiment variables: Augmentation type and level of loop gain; pilot location relative to the center of rotation for elevator commands; lag and time delay in the command path; and slow thrust response coupled with backside aerodynamic characteristics. Neither the MIL-F-8785C requirements nor any of several proposed requirements for pitch and control system dynamics were capable of correlating the experiment results without significant modification or extension.

2) The pitch rate augmentation system was generally preferred over the angle-of-attack augmentation. This was due to the lower turbulence response, attitude-hold feature, and trimmed pitch forces in level turns.

3) The pilot ratings were degraded for the cases where the pilot was located near or behind the center of rotation.

4) The evaluation pilots tended to apply a less demanding standard of maneuverability than for previous landing approach studies because the configurations were defined to be very large, 1 million lb, class III aircraft. The closed-loop pitch attitude bandwidth requirement for the landing approach task with this class of aircraft appears to be 1.5 rad/s.

5) The degradation caused by time delay was less severe than in previous landing approach studies. This is primarily a result of the decreased bandwidth demanded by the pilots for this class airplane. Data are presented which suggest that the amount of time delay that can be tolerated in the command path is inversely related to the dynamic bandwidth required to perform the task.

6) When the pilot position is forward of the center of rotation, the pitch acceleration response to control provides an early linear acceleration cue that is easily perceived by the pilot and confirms that the airplane is responding to his command. This effect may contribute to the higher tolerance to control system time delay observed in this experiment.

7) A multiloop analysis, which modeled an outer altitude control loop in series around the inner pitch-attitude loop, provided insight into the detrimental effects of locating the pilot aft of the center of rotation. A low-frequency closed-loop mode goes unstable at relatively low gain with the pilot aft of the center of rotation.

8) Evaluation of the Shuttle-like short aft tail configuration with the pilot located 10 ft behind the center of rotation was unacceptable when time lag and delay equal to that of the Shuttle was introduced into the pitch command path.

Acknowledgments

This research was sponsored by the U.S. Air Force Flight Dynamics Laboratory and NASA Dryden Flight Research Center under Contract F33615-79-C-3618.

References

[1] Weingarten, N. C. and Chalk, C. R., "In-Flight Investigation of Large Airplane Flying Qualities and Landing," AFWAL-TR-81-3118 and Calspan Report 6645-F-5, Dec. 1981.

[2] Reynolds, P. A., Wasserman, R., Fabian, G.J., Motyka, P.R., "Capability of the Total In-Flight Simulator," AFFDL-TR-72-39 and Calspan Report TB-3020-F-4, July 1972.

[3] Neal, T. P. and Smith, R. E., "An In-Flight Investigation to Develop Control System Design Criteria for Fighter Airplanes," AFFDL-TR-70-74 and Calspan Report BM-2821-F-4, June 1970.

[4] Smith, R. E., "Effects of Control System Dynamics on Fighter Approach and Landing Longitudinal Flying Qualities," Calspan Report AK-5280-12, March 1978.

[5] Radford, R. C., Smith, R. E., and Bailey, R. E., "Landing Flying Qualities Evaluation Criteria for Augmented Aircraft," Calspan Report 6339-F-3 and NASA CR-163097, Aug. 1980.

[6] Chalk,C. R., "Calspan Recommendations for Supersonic Cruise Aircraft (SCR) Flying Qualities Design Criteria," NASA CR-159236 and Calspan Report 6241-F-5, April 1980.

[7] DiFranco, D. A., "In-Flight Investigation of the Effects of Higher Order System Dynamics on Longitudinal Handling Qualities," AFFDL-TR-68-90 and Calspan Report BM-2238-F-4, July 1968.

[8] Schubert, G. R., "Digital Computer Program for Root Locus Analysis of Open-Loop Transfer Functions Containing e^{-TS} Lead-Lag Term," AFFDL-FDCC TM 65-43, Sept. 1965.

[9] Mooij, H. A., de Boer, W. P., and van Gool, M.F.C., "Determination of Low-Speed Longitudinal Maneuvering Criteria for Transport Aircraft with Advanced Flight Control Systems," National Aerospace Laboratory (NLR), the Netherlands, NLR TR79127u, Dec. 1979.

[10] Cooper, G. E. and Harper, R. P., "The Use of Pilot Rating in the Evaluation of Aircraft Handling Qualities," NASA TN D-5153, April 1969.